

A Well-Balanced Flow Equation for Noise Removal and Edge Detection

Celia Aparecida Zorzo Barcelos, Maurílio Boaventura, and Evanivaldo Castro Silva, Jr

Abstract—In this paper, an anisotropic nonlinear diffusion equation for image restoration is presented. The model has two terms: the diffusion and the forcing term. The balance between these terms is made in a selective way, in which boundary points and interior points of the objects that make up the image are treated differently. The optimal smoothing time concept, which allows for finding the ideal stop time for the evolution of the partial differential equation is also proposed. Numerical results show the proposed model's high performance.

Index Terms—Diffusion equation, edge detection, image processing, noise removal.

I. INTRODUCTION

THE use of partial differential equations (PDE) in image processing has grown significantly over the past years. The basic idea is to deform an image, a curve or a surface with a partial differential equation and obtain the expected results as a solution to this equation. One of the main advantages of the usage of partial differential equations is that it takes the image analysis to a continuous domain simplifying the formalism of the model, which becomes independent from the grid used in the discrete problem. Hence, an image can be defined as being an intensity function u given in each point $x \in \mathbb{R}^p$, $p = 2$ or 3 .

Given an image $u(x)$, one of the most common problems is to remove undesired interferences. We call the process for reconstruction the recovery process, where a given image in its initial data state contains errors, which are called "noise". The problem of reconstruction of images occurs, for example, in:

- medical images, as CT (transmission computed tomography), MRI (magnetic resonance imaging), MSI (magnetic source imaging), X-Ray, ESI (electrical source imaging), etc.;
- signals obtained via satellites;
- signals obtained from ocean depths;
- images obtained from airplanes to detect military targets, and others.

In general, the obtained signals have several errors and need to pass through "filters". A widely used method for noise elimination is the Gaussian filter, in which signals, in one and two

dimensions, are smoothed out by the convolution of the image with a Gaussian kernel. Nonetheless, the Gaussian operator is isotropic and therefore smoothes the image in all directions blurring sharp boundaries.

The goal in this work is to develop the idea of removing noise without losing the boundaries or edges. Many techniques have been introduced to improve the idea of Gaussian filters (see, e.g., [1], [2], [4]–[7], [11], [13], [15], [18] and [20]).

In order to attain this goal we will combine the ideas introduced in [11] and improved in [2] with the introduction of a forcing term that acts in the equation in a differentiated way on edge points and on interior points of the objects that are contained in an image.

II. THE MODEL

In this section we describe the proposed model relating it to the existent literature.

A. Segmentation and Noise Elimination—Modeling

Let I be an observed image and u the representation of the reconstructed image. These functions can be defined as functions of $\Omega \subset \mathbb{R}^2 \rightarrow \mathbb{R}$ that associate the pixel $(x, y) \in \mathbb{R}^2$ to its grayscale levels $I(x, y)$ or $u(x, y)$; Ω is the image support (generally, a rectangle).

The edges are defined as being the curves where the gradient obtains its local maximum. Therefore, if the received signal of an image is very noisy, the gradient will have a great number of irrelevant maxima that should be eliminated.

The simplest model based in PDE is a linear filter ([10], [12], and [18]) arranged by the convolution of signal I with a Gaussian function $G_\sigma = C_1 \sigma^{-1} \exp[-(x^2 + y^2)/2\sigma^2]$, where C_1 and σ are constants, $(x, y) \in \mathbb{R}^2$, i.e., the solution of the heat equation

$$u_t = \Delta u, \quad \text{in } \Omega \times \mathbb{R}_+, \quad u(x, y, 0) = I(x, y)$$

where $\Omega \subset \mathbb{R}^2$ is the image's domain.

This is equivalent to the flow equation associated to the decrease of the gradient for the energy functional $E(u) = \int_\Omega |\nabla u|^2 dx$.

Nonetheless, we cannot preserve the localization of the image edges by using this isotropic diffusion. This diffusion smoothes out everything in an image.

An important contribution for edge preservation was introduced by Malik and Perona [11]. They substituted the heat equation by the following anisotropic diffusion equation:

$$u_t = \text{div}(g(|\nabla u|) \nabla u), \quad \text{in } \Omega \times \mathbb{R}_+ \\ u(x, y, 0) = I(x, y) \quad (2.1)$$

Manuscript received April 26, 2002; revised January 6, 2003. This work was supported in part by CAPES. The associate editor coordinating the review of this manuscript and approving it for publication was Dr. Nicolas Merlet.

C. A. Z. Barcelos is with the FACOM-Federal University of Uberlândia-Uberlândia-MG and CAC-Federal University of Goiás-Catalão-GO (e-mail: celiabz@ufu.br).

M. Boaventura and E. C. Silva, Jr. are with the DCCE-IBILCE-UNESP-São José do Rio Preto-SP (e-mail: maurilio@dcce.ibilce.unesp.br; evanivaldojr@hotmail.com).

Digital Object Identifier 10.1109/TIP.2003.814242

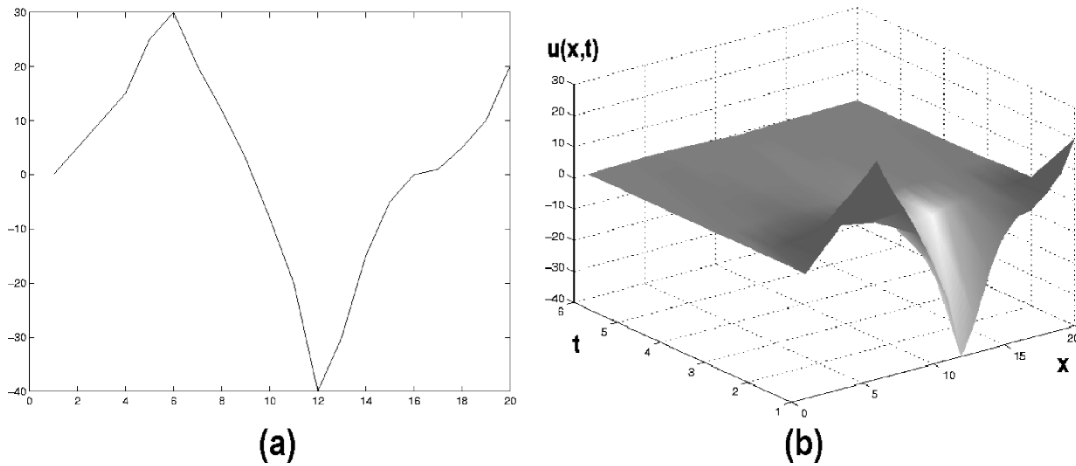


Fig. 1. Unidimensional signal (a) and its scale space (b).

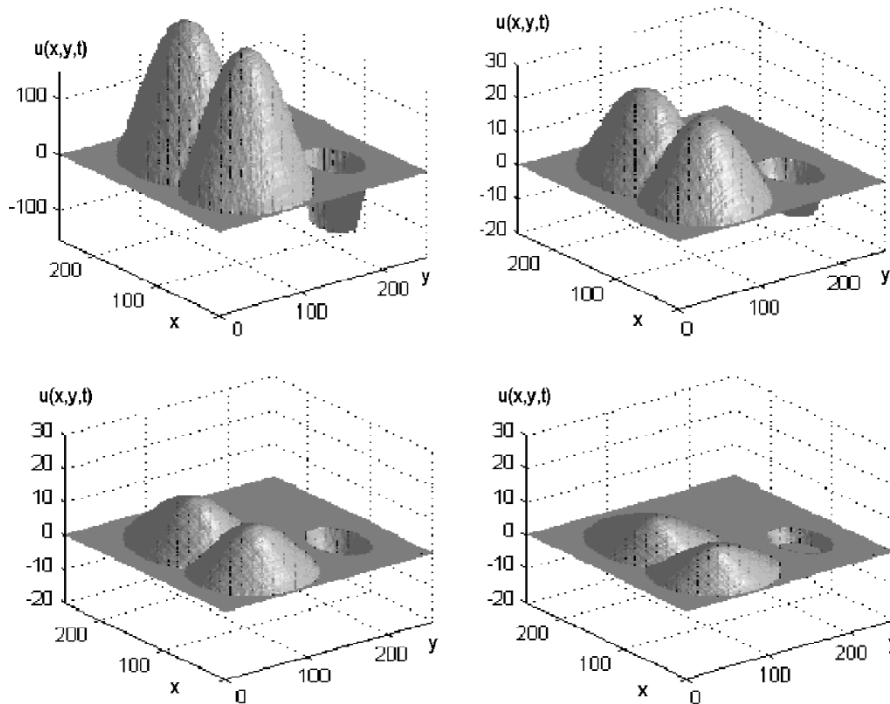


Fig. 2. Convolution of the signal $I * G_\sigma$ with the Gaussian function G_σ (3.2) for $t = 0, 0.5, 1.0$ and 2.0 (left to right, top to bottom).

where g is a nonincreasing, smooth function, such that $g(0) = 1$, $g(s) \geq 0$, and $g(s) \rightarrow 0$ when $s \rightarrow \infty$. The idea is that if $|\nabla u|$ is large, then the diffusion will be low, and therefore the exact localization of the edges will be preserved.

Computational experiments show that the “edge detector” based on this theory yields edges and boundaries that remain more stable through scale t . In spite of this, this model still has several theoretical and practical difficulties. For instance, if the image is very noisy, the gradient $|\nabla u|$ will be very large, and as a result, the function g will be close to zero at almost every point. Consequently, almost all noise will remain when we use the smoothing process introduced by this model.

From a geometric point of view, we can modify the diffusion operator in a way that the diffusion process becomes more intense along the edges and less intense along the perpendicular direction of the edges.

The following degenerated diffusion equation

$$u_t = |\nabla u| \operatorname{div} \left(\frac{\nabla u}{|\nabla u|} \right)$$

known as “mean curvature flow” achieves this objective and has the following geometric interpretation: the level lines of the solution propagate in the normal direction with speed proportional to the mean curvature.

Combining this idea of degenerated diffusion with the idea given by Malik-Perona [11], to substitute $|\nabla u|$ by $|\nabla G_\sigma * u|$ in the mean curvature flow equation, Alvarez, Lions, and Morel [2] proposed and studied the following model:

$$u_t = g(|\nabla G_\sigma * u|) |\nabla u| \operatorname{div} \left(\frac{\nabla u}{|\nabla u|} \right) \quad (2.2)$$

$$u(x, y, 0) = I(x, y) \quad (2.3)$$

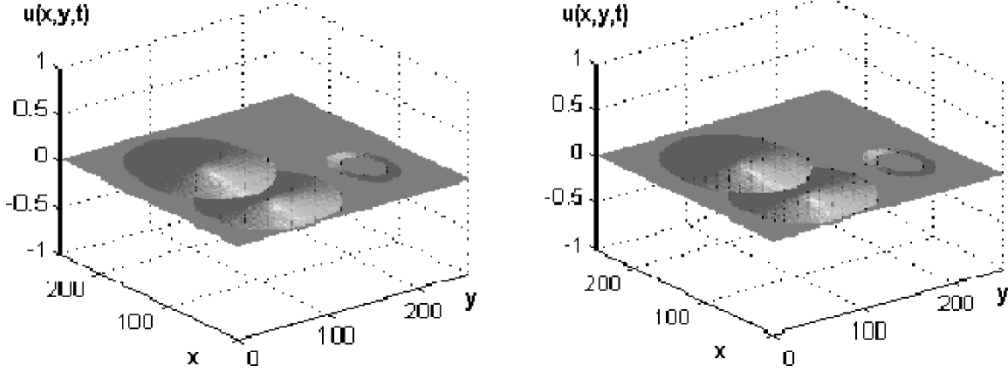


Fig. 3. Convolution of the signal $I(x, y)$ (Fig. 2) with the Gaussian function (3.4) for the values of (a) $a = 2$ and (b) $a = 100$.

$$\left. \frac{\partial u}{\partial n} \right|_{\partial\Omega \times \mathbb{R}_+} = 0 \quad (2.4)$$

which has a superior performance if compared to the methods already described; yet it still destroys sharp corners. In this paper we will refer to this model as the ‘‘ALM-model’’.

A fact that should be highlighted here is the modification proposed by Nordström [14], which points toward the introduction of the forcing term $(u - I)$ in the Malik-Perona (2.1) resulting in the model

$$\frac{\partial u}{\partial t} - \operatorname{div}(g(\nabla u)\nabla u) = I - u. \quad (2.5)$$

This new term has the property of preserving $u(x, y, t)$ close to the initial image $I(x, y)$.

In addition, the above equation has the advantage of possessing a nontrivial stationary state [2] eliminating, in this way, the necessity of a selection process for stop time.

As observed in [2], we can insert the forcing term $u - I$ in (2.2) without altering the theoretical results already obtained.

The presence of the forcing term $(u - I)$ in (2.1) and (2.2) reduces the degenerative effects of the diffusion to very acceptable levels; however, the models with this forcing term do not eliminate noise satisfactorily.

In this paper, following the ideas in [2], [3], [11], and [14], we propose the following parabolic equation for image restoration:

$$\begin{aligned} u_t &= g|\nabla u| \operatorname{div} \left(\frac{\nabla u}{|\nabla u|} \right) - \lambda(1-g)(u-I), \\ &\quad x \in \Omega, \quad t > 0, \\ u(x, y, 0) &= I(x, y), \quad x \in \Omega \\ \left. \frac{\partial u}{\partial n} \right|_{\partial\Omega \times \mathbb{R}_+} &= 0, \quad x \in \partial\Omega, t > 0 \end{aligned} \quad (2.6)$$

where $g = g(|G_\sigma * \nabla u|)$, $I(x, y)$ is an image to be processed, $u(x, y, t)$ is its smoothed version in the scale ‘‘ t ’’, G_σ is a convolution kernel (here, a Gaussian function), and $G_\sigma * \nabla u$ is the local estimate of ∇u used for noise elimination. The function $g(s) \geq 0$ is a nonincreasing function, satisfying $g(0) = 1$ and $g(s) \rightarrow 0$ when $s \rightarrow \infty$.

The term $|\nabla u| \operatorname{div}(\nabla u / |\nabla u|) = \Delta u - \nabla^2 u(\nabla u, \nabla u) / |\nabla u|^2$ diffuses u in the orthogonal direction to its gradient ∇u and does not diffuse it in any other direction. The goal is to allow

smoothing in the image u in a way that it is made on both sides of an edge with minimal smoothing on the edge itself.

The term $g(|G_\sigma * \nabla u|)$ is used for edge detection and controls the diffusion speed: if ∇u has a small mean in a neighborhood of a point x , it will be considered an interior point, and the diffusion will be stronger; on the other hand, that is, if ∇u has a large mean value in the neighborhood of x , then this point x will be considered an edge point, and the diffusion will be low since $g(s)$ assumes considerably smaller values for large values of s .

The balance between the forcing term and the diffusion term is made by $(1 - g)$, which works as a moderated selector of the diffusion process. Thus, the proposed model consists of selectively applying the ALM model in areas of the image that demand a larger suavization. This model also consists of forcing, in an incisive way, the smoothed image u to remain close to the initial image I in the boundary areas which have $g \sim 0$. On the other hand, in homogeneous areas $g \sim 1$, and therefore, the forcing term will have an inexpressive effect, which allows for a better suavization of the image.

The convolution $G_\sigma * \nabla u$ defines a ‘‘Gaussian scale space.’’

III. GAUSSIAN SCALE SPACE

Definition: Let $g : \mathbb{R}^n \rightarrow \mathbb{R}$. The Gaussian scale space of g is a function $T_g : \mathbb{R}^n \times \mathbb{R}_+ \rightarrow \mathbb{R}$, given by

$$T_g(x, t) = g * G_t(x),$$

where

$$G_t(x) = \frac{1}{(2a\pi t)^{\frac{n}{2}}} e^{-\frac{(x_1^2 + \dots + x_n^2) - \mu}{2at}} \quad (3.1)$$

is the Gaussian distribution of dimension n with mean μ and variance at , where a is a positive constant. The standard deviation is $\sigma = \sqrt{at}$ and $x = (x_1, \dots, x_n) \in \mathbb{R}^n$. The parameter t is called the scale.

In literature, many authors, for instance [2], [5] and [15], consider σ a selected parameter, the mean $\mu = 0$ and the constant $a = 2$. Encouraged by (3.1) and by the selection of the mean $\mu = 0$, we consider, in this work, σ as the standard deviation of the noise, which has zero mean in the Gaussian distribution. We do not fix the constant a , for convenience sake, which will become clearer further in the text.

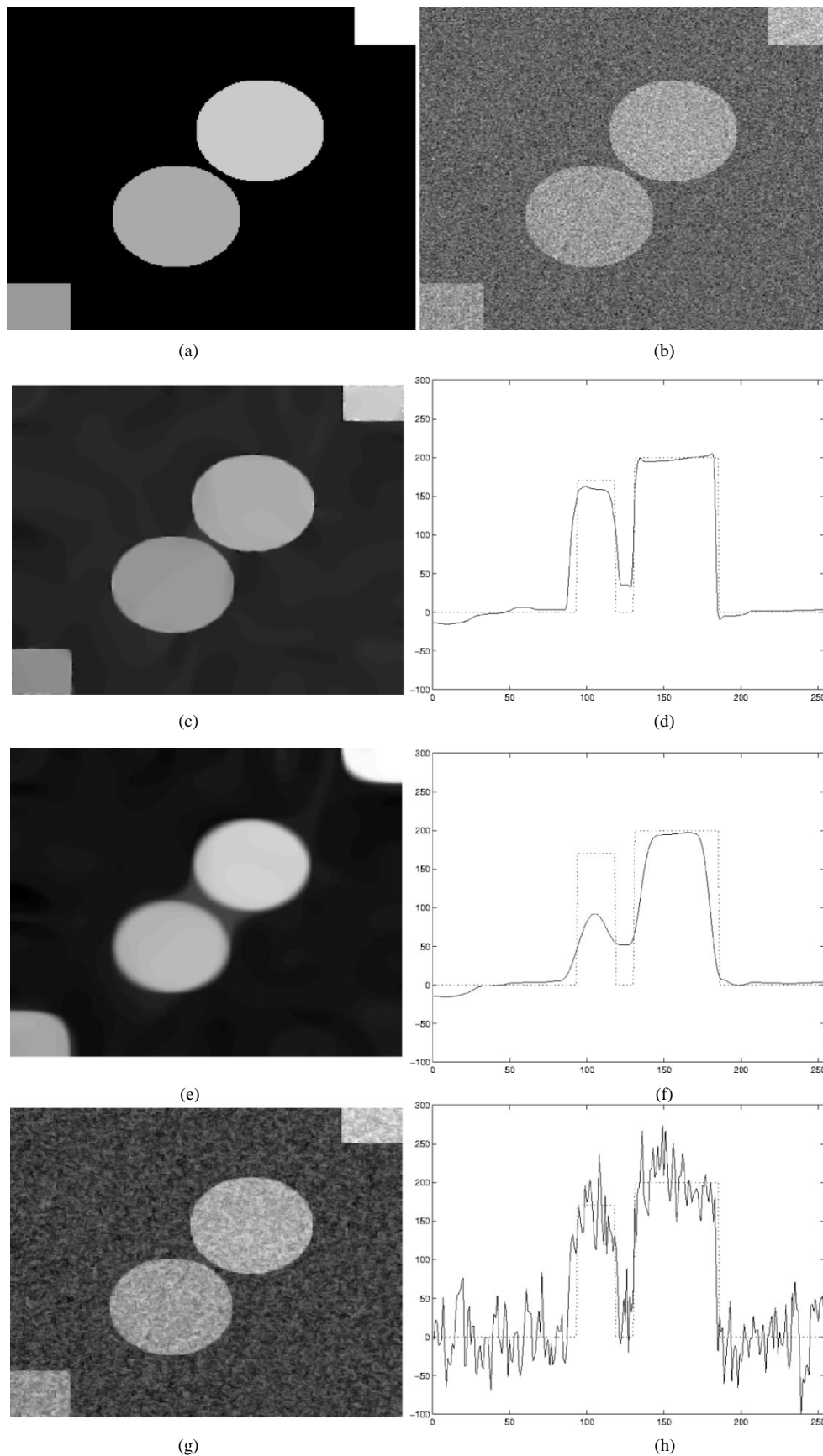


Fig. 4 (a) Original and (b) noisy image $\text{SNR} = 0$ db. (c) Reconstructed image by the proposed model and (d) line plot of the 128th row. (e) Reconstructed image by the ALM model and (f) line plot of the 128th row. (g) Reconstructed image by ALM-modified model and (h) line plot of 128th row.

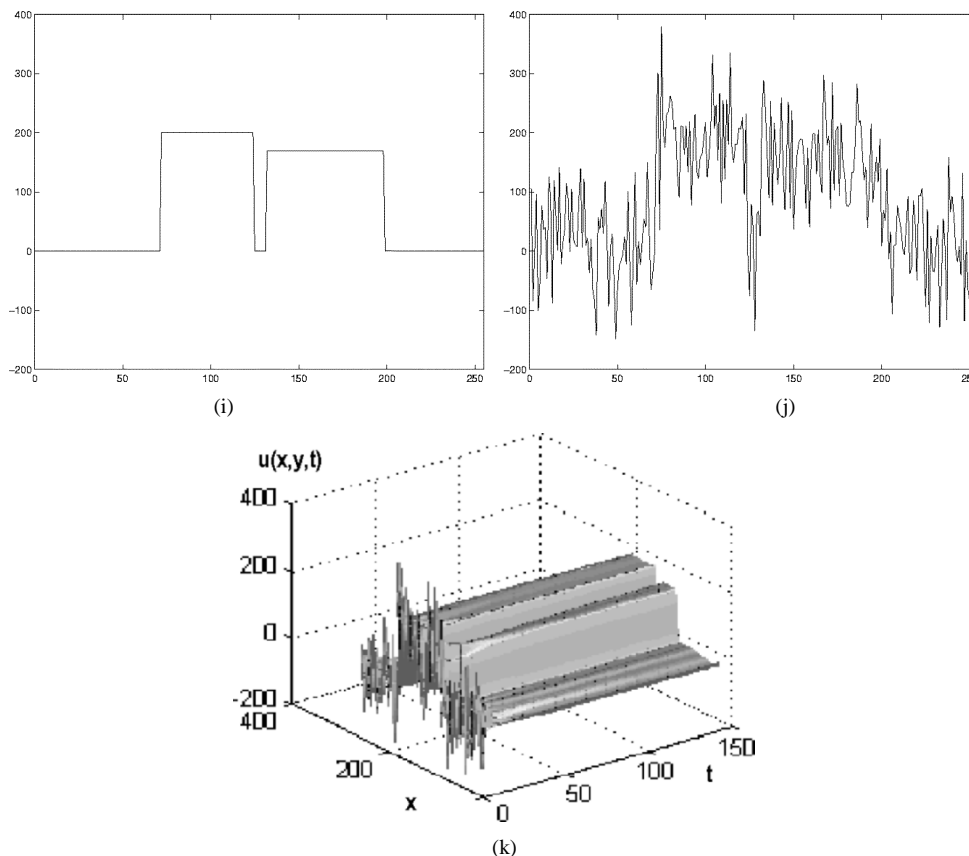


Fig. 4 (Continued.) Line plots of the 128th (i) original and (j) noisy. Scale space for the lines $y = 128$ of the signal in Fig. 4(j). (k) Scale space for Fig. 4(j).

The Gaussian scale space has important properties as invariance by translation and rotation, semi-group property, and causality, among others ([11] and [17]).

The Gaussian scale space $T_I(x, t) = I * G_t(x)$ is the heat equation solution $u_t = \Delta u$ at time t , with $u(x, 0) = I(x)$.

In other words, the scale space of a signal is the composition of this signal convoluted with Gaussians of all possible variances, that is, $t \rightarrow \infty$.

In Fig. 1(b), we have the scale space for the signal in Fig. 1(a) with

$$G_t(x) = \frac{1}{(4\pi t)^{\frac{1}{2}}} e^{-\frac{x^2}{4t}}. \tag{3.2}$$

There are techniques, in literature, to find the best value for σ . The desired value of σ is obtained using a scale space tracking technique ([8] and [19]). This procedure presents a high computational cost that makes it very nearly impractical.

In Fig. 2, we present the effect of the convolution of an image $I(x, y)$ with different values for the scale t , where $t = \sigma^2/2$.

We have observed that as the scale grows, the image gets more smoothed.

Let us suppose that the image shown in Fig. 2. is a noise that we want to eliminate. We need to find the scale that eliminates this noise. The greater the noise level is, the greater the value of t . Let's denote for T_o the value of t in which the noise level in the scale t is considered insignificant. As the amount of noise that we want to eliminate is directly related to the standard deviation of the noise σ , and the time t relates to the noise in the form $at = \sigma^2$, that is, the correspondent t scale for this smoothing level is

given by $t = \sigma^2/a$. Intuitively and experimentally affirmed, over a two year period with more than 300 trials on synthetic images with different levels of noise, between 15 db and -12 db, which have zero mean in the Gaussian distribution and also some trials on medical and real life images, we arrived at the following definition for the optimal time of smoothing.

Definition: The suavization optimal time needed to achieve an efficient and adequate suavization level in a noisy image with standard deviation of the noise σ is given by the expression

$$T_o = \frac{\sigma^2}{a} \tag{3.3}$$

where a is a constant present in the Gaussian kernel

$$G_t(x) = \frac{1}{2a\pi t} e^{-\frac{|x|^2}{2at}}, \quad x \in \mathbb{R}^n. \tag{3.4}$$

The definition of the optimal smoothing time assumes that the σ value of Gaussian noise is known. It is true for synthetic images but not true for any industrial application, in this case the σ value should be estimated by taking reference from other images of the same type, where the noise standard deviation is known.

A. Mathematical Validity

As our equation for u is a nonlinear parabolic equation with degeneration possibilities, the discussion of our model's mathematical validity is in the sense of viscosity solutions [9]. The existence, uniqueness, and stability are based on the theory of viscosity solutions, which is based on the Maximum Principle.

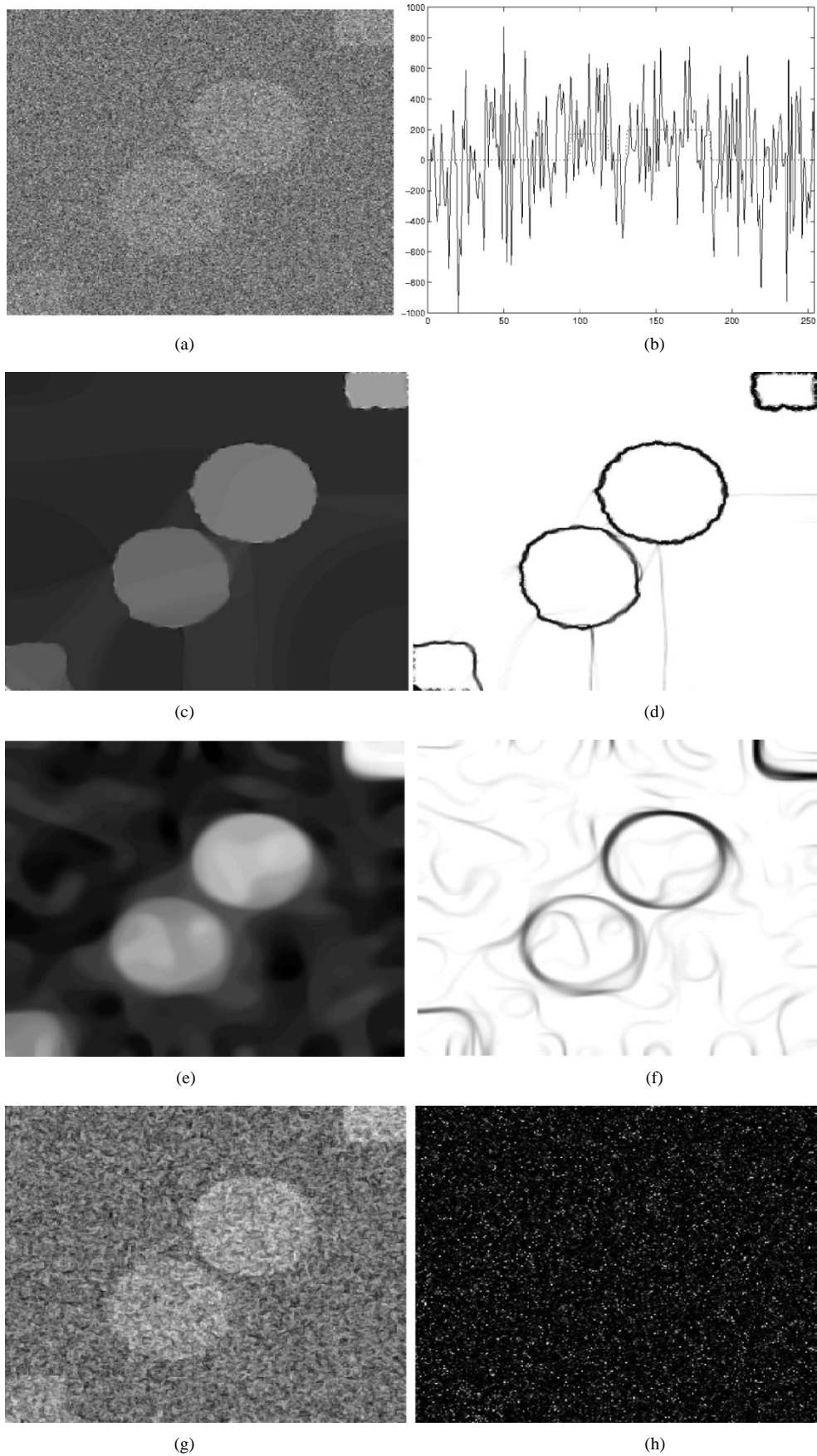


Fig. 5. (a) Noisy image $\text{SNR} = -12$ db and (b) plot of the 128th row line graph. Reconstructed image by the (c) proposed model and (d) segmentation. Reconstructed image by the (e) ALM model and (f) its segmentation. Reconstructed image by (g) the ALM-modified model and (h) segmentation.

The proposed equation is in two dimensions, yet we can study this problem for the n -dimensional case. To simplify the notation we can consider, in the theoretical part, the constants σ , λ and k as $\sigma = \lambda = k = 1$ and work with periodic boundary conditions. Then, by periodic extension, we consider the following Cauchy problem:

$$\begin{aligned} \frac{\partial u}{\partial t} &= g a_{ij} (\nabla u) u_{x_i x_j} - (1 - g)(u - I), \quad x \in \mathbb{R}^n, \\ t &\in \mathbb{R}_+, \quad u(x, 0) = I(x), \quad x \in \mathbb{R}^n \end{aligned}$$

where

$$\begin{aligned} g &= g(s) = \frac{1}{1 + |s|^2}, \quad s = (s_1, \dots, s_n) = \nabla G * u, \\ \frac{\partial g}{\partial l} &= \frac{\partial g}{\partial s_l}(s), \quad G = \frac{1}{(4\pi)^{\frac{n}{2}}} \exp\left\{-\frac{|x|^2}{4}\right\}, \\ a_{ij}(p) &= \delta_{ij} - \frac{p_i p_j}{|p|^2}. \end{aligned} \quad (3.5)$$

Definition: Let $u \in C(\mathbb{R}^n \times [0, T])$ for some $T > 0$. A solution u of (3.5) is said to be a *viscosity sub-solution* if, for any $\phi \in C^2(\mathbb{R}^n \times \mathbb{R})$ and for any point $(x_0, t_0) \in \mathbb{R}^n \times (0, T]$, where $(u - \phi)$ assumes a local maximum, the following conditions are satisfied:

$$\begin{aligned} \frac{\partial \phi}{\partial t}(x_0, t_0) - g((\nabla G * u)(x_0, t_0)) \times \\ a_{ij}(\nabla \phi(x_0, t_0)) \phi_{x_i x_j}(x_0, t_0) - \\ (1 - g((\nabla G * u)(x_0, t_0))) [(u - I)(x_0, t_0)] \leq 0, \\ \text{if } \nabla \phi(x_0, t_0) \neq 0 \end{aligned} \quad (3.6)$$

$$\begin{aligned} \frac{\partial \phi}{\partial t}(x_0, t_0) - (g((\nabla G * u)(x_0, t_0))) \times \\ \limsup_{p \rightarrow 0} a_{ij}(p) \phi_{x_i x_j}(x_0, t_0) \leq 0, \\ \text{if } \nabla \phi(x_0, t_0) = 0. \end{aligned} \quad (3.7)$$

A viscosity super-solution is similarly defined substituting “local maximum” for “local minimum,” “ ≤ 0 ” for “ ≥ 0 ,” and “lim sup” for “lim inf” in the (3.6) and (3.7), respectively.

To show that the model is well posed, the same procedure given in [4] will be followed—approximate the solution u by approximated u^ϵ solutions, differentiate estimates, and prove the existence and uniqueness in the sense of viscosity solutions, applying the Maximum Principle, the estimates found, and the ideas developed in [2].

Theorem: The Cauchy problem (3.5) has a unique viscosity solution $u \in C(\mathbb{R}^n \times [0, T]) \cap L^\infty(0, T; W^{1,\infty}(\mathbb{R}^n))$ for any $T \in [0, \infty)$, and also, $\inf_{\mathbb{R}^n} I \leq u(x, t) \leq \sup_{\mathbb{R}^n} I$, being I a continuous Lipschitzian function. In addition, if $v \in C(\mathbb{R}^n \times \mathbb{R}_+)$ is a viscosity solution of (3.5) with I substituted by a continuous function I_1 , then, for all $T \in [0, +\infty)$, there is a constant $C > 0$, depending only on I , I_1 , and T , such that

$$\sup_{0 \leq t \leq T} \|u(x, t) - v(x, t)\|_{L^\infty(\mathbb{R}^n)} \leq C \|I - I_1\|_{L^\infty(\mathbb{R}^n)}.$$

IV. NUMERICAL IMPLEMENTATION AND EXPERIMENTAL RESULTS

We here present some results obtained with the application of the described models in the previous sections in a synthetic,

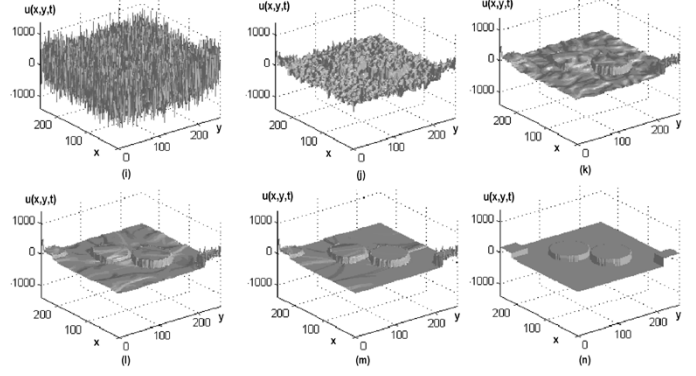


Fig. 5. (Continued.) Cross sections of the scale space for the surface given in Fig. 5(a) for $t = 0$ (i), $t = 0.8$ (j), $t = 4.0$ (k), $t = 20.0$ (l), $t = 916.3$ (m) and (n) for the surface given in Fig. 4(a) (original).

medical, and daily life image, which presents several complexity levels. We will call the “proposed model,” the model given by (2.6) and the “ALM-modified,” the model

$$\begin{aligned} u_t &= g(|\nabla G_\sigma * u|) |\nabla u| \operatorname{div} \left(\frac{\nabla u}{|\nabla u|} \right) - (u - I) \\ u(x, y, 0) &= I(x, y), \quad \text{and} \quad \frac{\partial u}{\partial n} \Big|_{\partial \Omega \times \mathbb{R}_+} = 0 \end{aligned}$$

with the Gaussian function given by (3.4). We observe that the lower the value of the constant a in (3.4), the greater the optimal time defined by (3.3) will be, for instance, the scale space given in Fig. 2 has as an optimal time $T_o = 3026.4$ with $a = 2$, and the result of the convolution is given in Fig. 3(a).

Using the expression (3.4) for the Gaussian with $a = 100$, we obtain the same result with an optimal time $T_o = 60.5$ [see Fig. 3(b)].

We observe that with this selection, we have an adequate smoothing level without the need of using any tracking technique. In addition, the images obtained in Fig. 3(a) and Fig. 3(b) present the same values for the maximum and the minimum in the set of pixels that define the image, that is, $\min = -2.1 \times 10^{-3}$ and $\max = 4.8 \times 10^{-3}$.

The images used are generally represented by 256×256 matrices where each matrix element $u_{i,j}$ is a real value correspondent to the grayscale level of the image $u(x, y)$ at the point $x = x_i = i\Delta x$ and $y = y_j = j\Delta y$. We denote $u(x_i, y_j, t_n)$ by $u_{i,j}^n$, where $t_n = n\Delta t$.

The derivative of u in relation to the time, that is, u_t calculated in (x_i, y_j, t_n) is approximated by Euler’s method, i.e., $u_t \sim ((u_{i,j}^{n+1} - u_{i,j}^n)/(\Delta t))$ and the diffusion term

$$|\nabla u| \left(\operatorname{div} \left(\frac{\nabla u}{|\nabla u|} \right) \right) = \frac{u_x^2 u_{yy} - 2u_x u_y u_{xy} + u_y^2 u_{xx}}{u_x^2 + u_y^2}$$

is approximated using central differences.

Implementing the diffusion (2.6) presents no difficulties and is straightforward (further details see [2], [4], [11] and [15]).

The models, ALM, ALM modified and proposed model, all present the same computational complexities once the diffusion term—which is the term of greater order in the differential equation which define them—is the same for all three models.

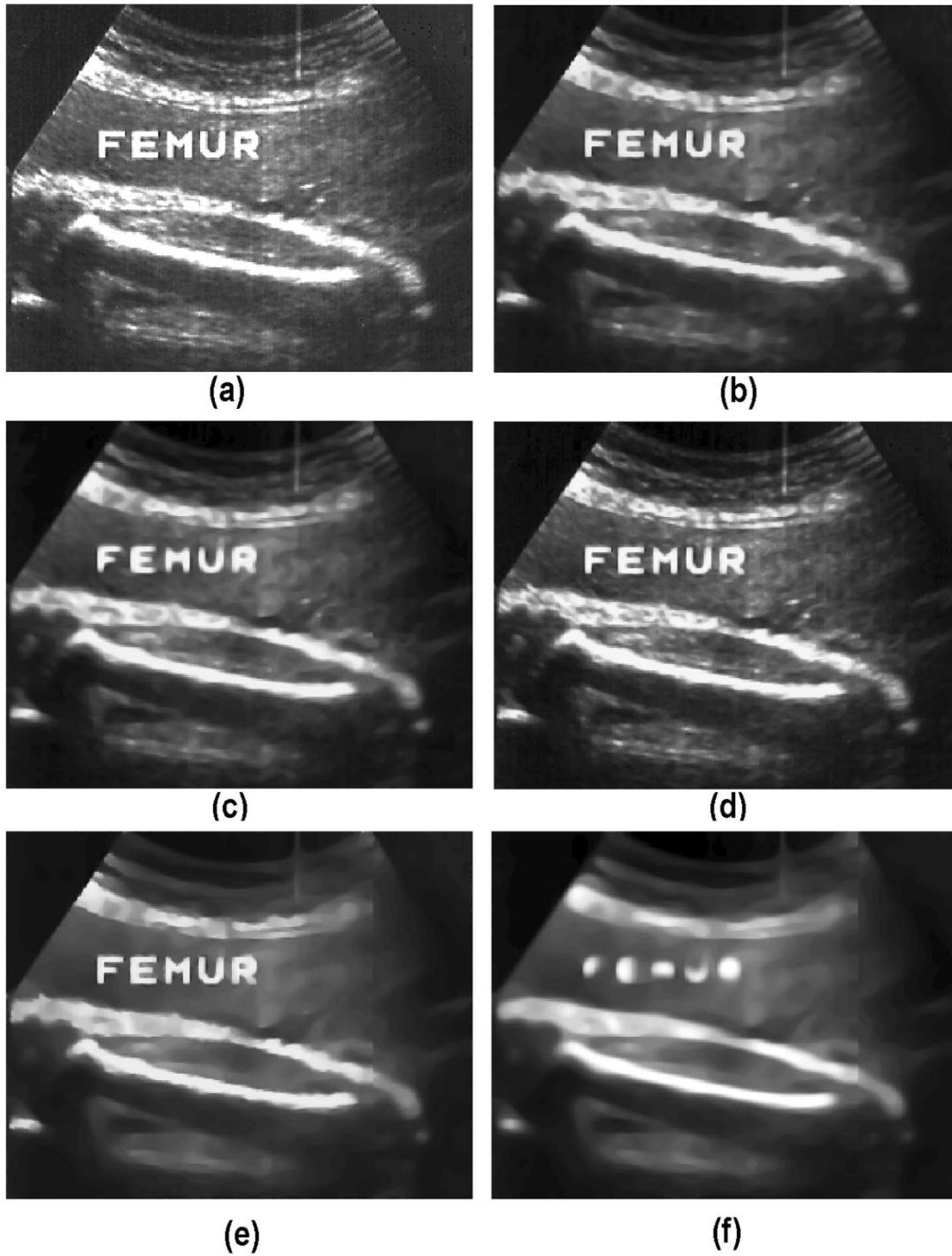


Fig. 6. Ultrasonography of (a) femur original, (b) proposed model, (c) ALM model, and (d) ALM-modified model. Image reconstructed by (e) the proposed model and by (f) the ALM model with 100 iterations.

Using Neumann's boundary conditions we calculate u_{ij}^{n+1} , $n = 1, 2, \dots, N$, by

$$u_{ij}^{n+1} = u_{ij}^n + \Delta t \mathcal{L}(u_{ij}^n) \quad (4.1)$$

with $u_{ij}^0 = I(x_i, y_j)$ and

$$\mathcal{L}(u) = g|\nabla u| \operatorname{div} \left(\frac{\nabla u}{|\nabla u|} \right) - \lambda(1-g)(u-I).$$

In all experiments we took $\lambda = \sigma_r$, $g = g(|G_{\sigma_r} * \nabla u|) = (1/(1+k|G_{\sigma_r} * \nabla u|^2))$, k as an I dependent constant and σ_r as the standard deviation of the noise in I .

Until the present, there are no rigorous choices for the values of k . In practice the k constant was chosen in a manner which allows the function $g(s)$ to carry out its role which is $g \sim 0$ when s is large (edge points) and $g \sim 1$ when s is small (interior points).

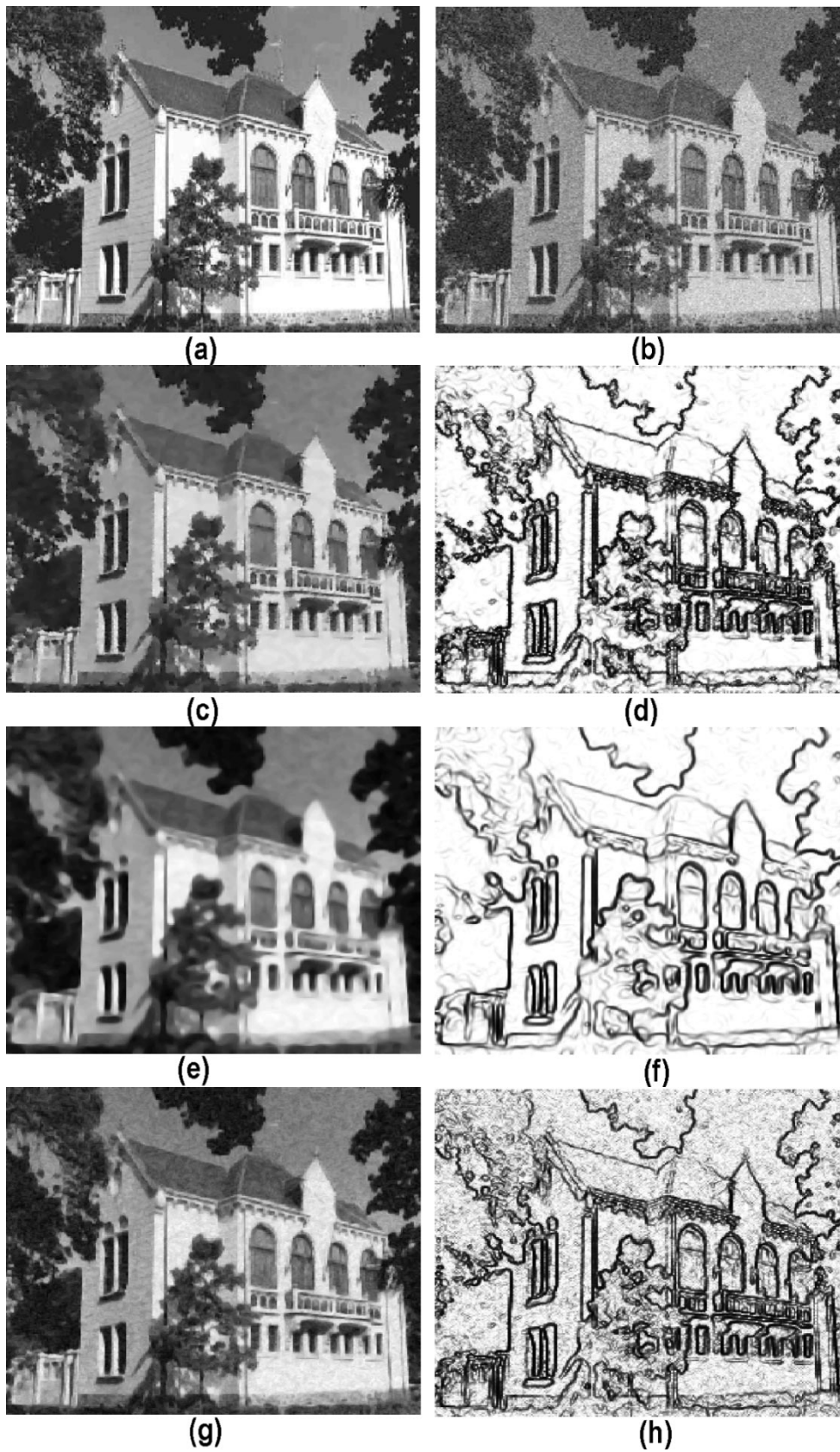


Fig. 7. (a) Original image and (b) noisy image—SNR = 12 db. (c) Image reconstructed by the proposed model and (d) its segmentation. (e) Image reconstructed by the ALM model and (f) its segmentation. (g) Image reconstructed by the ALM-modified model and (h) its segmentation.

The results of the concluded tests are presented at time $t = T_o$, considering the optimal time $T_o = \sigma_r^2/100$. The optimal

time is directly related to the noise intensity (σ_r), so for highly-level noisy images, a longer time of evolution in the scale “ t ”

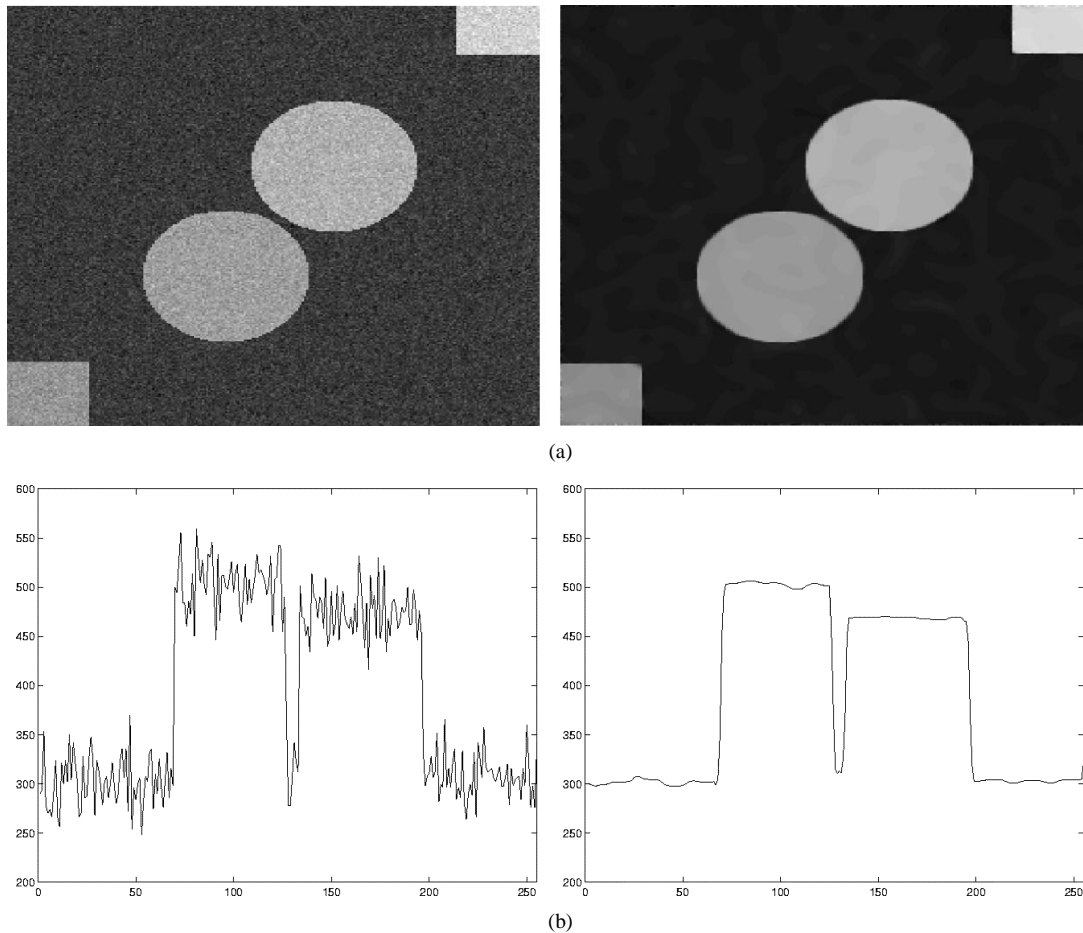


Fig. 8. (a) Poisson noisy image (SNR = 11 db) and reconstructed image by proposed model. (b) Line plots of the 130th noisy and smoothed rows, respectively.

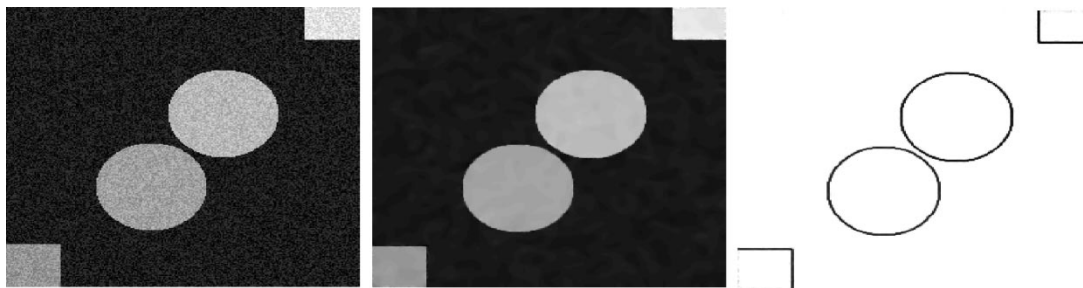


Fig. 9. Degraded image by uniform noise (SNR = 11 db), image reconstructed by the proposed model and its edge-map.

will be necessary. On the other hand, the optimal time is related to the number of iterations N , that is, $T_o = N\Delta t$.

In the example given in Fig. 2, considering the standard deviation $\sigma_r = 77.8$ and $a = 2$ in (3.4) we obtain $T_o = 3026.4$ to achieve an ideal smoothing level. Considering $\Delta t = 0.1$ 30 264 iterations will be necessary, where in contrast we obtain $T_o = 60.5$, and only 605 iterations are needed with $a = 100$. This means a high computational gain.

We present the results obtained using different pictures. We selected the parameters that allow the best results for the ALM and ALM-modified model.

The original images (noiseless) are represented in many grayscale levels and although they present gray intensity levels

in the range from 0 to 255, the addition of noise to the intensity values is well outside the 0–255 range. For example, the noisy image shown in Fig. 5(a) contains pixels with intensities as low as -1200 and as high as 1400 . The noise levels (SNR) in each considered picture are shown on the respective legends. For the visualization of the images, we used Matlab.

Our first experiment (Fig. 4.) is an artificial image that contains geometric objects. The pictures in Fig. 4(a),(b) have the original and noisy images.

With the application of different models in Fig. 4(b), 141 iterations were run ($T_o = 56.7$) and the parameters $k = 1100$, $\sigma_r = 75.3$, and $\Delta t = 0.4$ were used. The results are shown in Fig. 4(c), (e), and (g). The graphs correspondent to the 128th

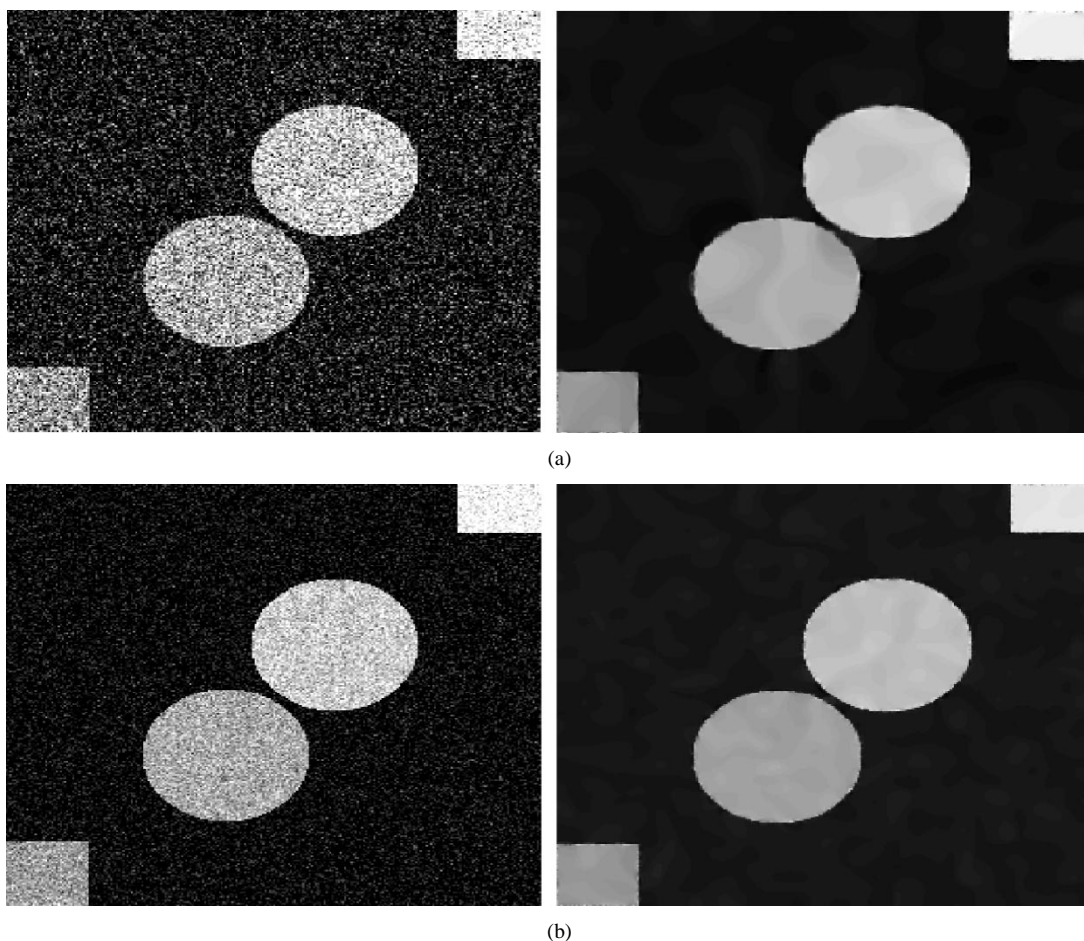


Fig. 10. (a) Degraded image by 3.5 db white noise, image reconstructed by the proposed model and its segmentation. (b) Degraded image by 9.5 db white noise, image reconstructed by the proposed model and its segmentation.

row plot in each case are also presented. The “dotted” line refers to the original picture whereas the “continuous” line refers to the smoothed image.

As can be observed, the application of several models to the presented image in this picture allows satisfactory results. However, the best result is that presented by the proposed model, as can be observed on the graph’s 128th row plot. We can notice that in Fig. 4(e) there are deformations on the edges, and in Fig. 4(g), the smoothing level was not intense enough.

In Fig. 4 (i)-(k), we present the graph correspondent to the 128th row plot of the noiseless image Fig. 4(a), the noisy image Fig. 4(b) and the scale space graph generated by the proposed model for this signal.

We can observe that the suavization degree obtained by the proposed model with 141 iterations is of very good quality.

Now, we consider the same image, yet with a higher intensity of noise level (Fig. 5).

In this case, 2291 iterations were run in the proposed model and in the ALM-modified model to achieve an optimal time ($T_o = 916.3$). In the ALM model, only 100 iterations occurred because there was a progressive deformation of the edges, which would result in a total destruction of the image if we were to take the same number of iterations as that of the other models. The parameters used in this case were $k = 34500$, $\Delta t = 0.4$ and $\sigma_r = 302.7$.

This example illustrates the good performance of the proposed model as observed in the smoothed images and their respective segmentations. Only the proposed model achieved satisfactory results. The ALM model presents edge losses, and the smoothing level in the ALM-modified model is very low, which does not allow for an adequate segmentation.

Another way of noting the high performance of the proposed model is through observing the scale space generated by (2.6).

We can note from the surface graphs shown in Fig. 5(i)-(n) (generated for many values of the scale t) that in the initial scale ($t = 0$) the noise in the initial image makes the detection of any shape impossible because of the entanglement of “peaks” resulted by the high noise level (SNR = -12 db). But even so, when we apply the proposed model, we can eliminate practically almost all the noise without losing the edges, which can be confirmed when we compare Fig. 5(m) (surface plot in $T_o = 916.3$) with Fig. 5(n) (original surface).

The next picture (Fig. 6) is a medical image of a fetal ultrasonography of a femur. In this case, we only have a noisy image acquired by an ultrasound device. We can observe that the noise level is very low. As the standard deviation is not known in this case, its value was estimated in $\sigma_r = 15.0$. The parameters used in this example were $k = 0.25$ and $\Delta t = 0.1$.

Only 22 iterations were required in this example to accomplish the diffusion’s optimal time. All models acted in similar

manners producing similar results as can be observed. The low level of noise justifies the good performance of all models. Although we can observe a subtle edge deformation in the ALM model and a lower smoothing degree in the ALM-modified model, and the fact that even though these factors do not significantly influence the visualization of the images, we perceive that the evolution of the process beyond the optimal time leads to a progressive deformation with the application of the ALM model [Fig. 6(f)], whereas the proposed model preserves the images characteristics allowing for a better image outline, as shown by the following pictures [Fig. 6(e)], which were generated after running 100 iterations.

The following example refers to a real life image (Fig. 7). This image presents high complexity by having different textures. The noise level was considered as SNR = 12 db. 32 iterations were run to achieve the optimal time ($T_o = 3.2$), and the parameters $k = 1000$, $\sigma_r = 17.9$ and $\Delta t = 0.1$. Once more, one can observe in the pictures shown below that the proposed model presents the best results. In the ALM model, we note an accentuated loss of edges and corners. Although the ALM-modified model presents good visual results, we observe in its segmentation that the smoothing level is not satisfactory if compared to the other two methods.

The feasibility of the proposed model was reached by testing a large group of images principally synthetic images, some everyday life and medical images all of which have different levels of noise and a zero mean Gaussian distribution. As well as these some images with noise of different origins such as Poisson noise, white noise and uniform noise were tested. In the following pictures we present some of the results from these images.

Different noise origins and different levels of noise, in the image presented in Fig. 4(a), were considered. Fig. 8(a) shows the Poisson noisy version (SNR = 11 db) and the reconstructed image obtained by the proposed model after 30 iterations. The parameters used are: $k = 57$, $\sigma_r = 24.5$ and $\Delta t = 0.2$. Fig. 8(b) shows the line plots of the 130th row. Fig. 9 shows the noisy version (SNR = 11 db) obtained by adding uniform noise and the smoothed image u obtained after 40 iterations with parameters: $k = 100$, $\sigma_r = 21.8$ and $\Delta t = 0.2$. In Fig. 10, two levels of white noise were considered. Fig. 10 shows the noisy version with SNR = 3.5 db (a) and SNR = 9.5 db (b) and the smoothed image obtained by the proposed model using the parameters $k = 415$, $\sigma_r = 49.7$, $\Delta t = 0.2$ for Fig. 10(a) and $k = 1000$, $\sigma_r = 25.7$ and $\Delta t = 0.2$ for Fig. 10(b). Fig. 10(c) shows the map of the edges of the smoothed images obtained in (a) and (b), respectively.

The computational code was written in C language. The results were obtained by using a Pentium III PC (128 Mb RAM, 800 MHz). The running time for an image of 256×256 pixels size was about 20 s for each set of 100 iterations.

V. CONCLUSIONS

One can conclude, by considering the given examples, that the proposed model presented a better performance in all aspects, producing images with a high quality of segmentation and efficient smoothing compared to the other presented models.

Apart from the proposal of a new model, this work brings innovations such as the use of the parameter σ in the Gaussian function as being the noise standard deviation, whereas other authors refer to this variable as only a selected parameter, and the optimal time estimate in the process of temporal evolution.

The balanced smoothing and the use of the optimal time concept to stop the evolution of the partial differential equation produces good results and a high computational gain in noise removal and in the image edge detection process.

ACKNOWLEDGMENT

The authors would like to thank the referees for their useful remarks on the first version of the manuscript.

REFERENCES

- [1] L. Alvarez and J. Esclarim, "Image quantization using reaction-diffusion equations," *SIAM J. Appl. Math.*, vol. 1, no. 57, pp. 153–175, 1997.
- [2] L. Alvarez, P. L. Lions, and J. M. Morel, "Image selective smoothing and edge detection by nonlinear diffusion," *SIAM J. Numer. Anal.*, vol. 29, no. 3, pp. 845–866, 1992.
- [3] C. A. Z. Barcelos, *Edge-Preserving Regularization in Image Restoration*, 2002.
- [4] C. A. Z. Barcelos and Y. Chen, "Heat flows and related minimization problem in image restoration," *Comput. Math. Applicat.*, no. 39, pp. 81–97, 2000.
- [5] F. Catté, T. Coll, P. L. Lions, and J. M. Morel, "Image selective smoothing and edge detection by nonlinear diffusion," *SIAM J. Numer. Anal.*, vol. 29, pp. 182–193, 1992.
- [6] A. Chambolle and P. L. Lions, "Image recovery via total variation minimization and related problems," *Numer. Math.*, vol. 76, pp. 167–188, 1997.
- [7] Y. Chen, C. A. Z. Barcelos, and B. A. Mair, "Smoothing and edge detection by time-varying coupled nonlinear diffusion equations," *Comput. Vis. Image Understand.*, vol. 82, no. 2, pp. 85–100, 2001.
- [8] Y. Chen, B. C. Vemuri, and L. Wang, "Image denoising and segmentation via nonlinear diffusion," *Comput. Math. Applicat.*, vol. 39, no. 5/6, pp. 131–149, 2000.
- [9] M. G. Crandall, H. Ishii, and P. L. Lions, "User's guide to viscosity solutions of second order partial differential equations," *Bull. Amer. Math. Soc.*, vol. 27, no. 1, pp. 1–67, 1992.
- [10] J. J. Koenderink, "The struture of images," *Biol. Cybern.*, vol. 50, pp. 363–370, 1984.
- [11] J. Malik and P. Perona, "Scale-space and edge detection using anisotropic diffusion," *IEEE Trans. Pattern Anal. Machine Intell.*, vol. 12, no. 7, pp. 629–639, 1990.
- [12] D. Marr and E. Hildreth, "Theory of edge detection," in *Proc. R. Soc. Lond. B*, vol. 207, 1980, pp. 187–217.
- [13] J. M. Morel and S. Solimini, *Variational Methods in Image Segmentation*. Boston, MA: Birkhäuser, 1995.
- [14] K. N. Nordström, "Biased anisotropic diffusion: a unified regularization and diffusion approach to edge detection," *Image Vis. Comput.*, no. 8, pp. 318–327, 1990.
- [15] L. Rudin, S. Osher, and E. Fatemi, "Nonlinear total variation based noise removal algorithms," *Phys. D*, vol. 60, pp. 259–268, 1992.
- [16] J. A. Sethian, *Level Set Methods*. Cambridge, U.K.: Cambridge Univ. Press, 1996.
- [17] R. Teixeira, "Introdução aos Espaços de Escala," in *23º Colóquio Brasileiro de Matemática*. Rio de Janeiro: IMPA, 2001.
- [18] A. P. Witkin, "Scale-space filtering," in *Proc. IJCAI*, Karlsruhe, 1983, pp. 1019–1021.
- [19] G. Whitten, "Scale space tracking and deformable sheet models for computational vision," *IEEE Trans. Pattern Anal. Machine Intell.*, vol. 15, pp. 697–706, 1993.
- [20] Y. L. You and M. Kaveh, "Fourth-order partial differential equations for noise removal," *IEEE Trans. Image Processing*, vol. 9, pp. 1723–1730, Oct. 2000.



Celia Aparecida Zorzo Barcelos received the M.Sc. and Ph.D. degrees in mathematics from University of São Paulo (USP), Brazil, in 1984 and 1990.

She is a Professor at the Federal University of Uberlândia and the Federal University of Goiás. She held the position of Visiting Professor at the University of Florida from 1996 until 1998. Her research interests include nonlinear partial differential equations, inverse problems, numerical analysis; fields of application include image restoration, segmentation, motion estimation, and inpainting.

Dr. Barcelos is a member of the Deliberative Council of the Brazilian Society of Computational and Applied Mathematics.



Evanivaldo Castro Silva, Jr. received the B.Sc. degree in mathematics and the M.Sc. degree in computational and applied mathematics from São Paulo State University (UNESP), São José do Rio Preto-SP, Brazil, in 2000 and 2002, respectively.

His research interests include nonlinear partial differential equations, image restoration and segmentation, image analysis, parallel processing, and numerical analysis.



Maurílio Boaventura received the B.Sc. degree in mathematics from São Paulo State University (UNESP), São José do Rio Preto-SP, Brazil, in 1984, his M.Sc. degree in computer science and computational mathematics from University of São Paulo (USP), São Carlos-SP, in 1989, and the Ph.D. degree in applied mathematics from State University of Campinas (UNICAMP), Campinas-SP, in 1998.

His research interests include image analysis and restoration, parallel processing and numerical analysis. He is a Member of Staff with the Department of

Computing and Statistics (UNESP), São José do Rio Preto-SP, and is a member of the C.C.Complex at São Paulo State University (UNESP), Brazil.